

Adsorption Characteristics and Corrosion Inhibition Efficiency of Ethoxylated Octadecylamine Ionic Liquid in Aqueous Acid Solution

Ayman M. Atta^{1,2,*}, Gamal A. El-Mahdy^{1,3}, Hamad A. Allohedan¹ and Mahmood M. S. Abdullah¹

¹ Surfactants Research Chair, Department of Chemistry, College of Science, King Saud University, P.O. Box 2455, Riyadh 11451, Kingdom of Saudi Arabia.

² Petroleum Application Department, Egyptian Petroleum Research Institute, Cairo 11727, Egypt.

³ Department of Chemistry, Faculty of science, Helwan University, 11795 Helwan, Egypt.

*E-mail: aatta@ksu.edu.sa

Received: 9 October 2015 / *Accepted:* 30 November 2015 / *Published:* 1 January 2016

Ionic liquids attracted great attention as green surfactants to apply as corrosion inhibitors for steel in aqueous corrosive medium. In this work, amphiphilic ionic liquid was synthesized by quaternization of ethoxylated octadecylamine with p-toluene sulfonic acid to produce ODPEG-TS. The chemical structure was elucidated using NMR analysis. The surface activity of ODPEG-TS was measured from the relation between surface tension and different concentrations of ODPEG-TS in aqueous and acidic solutions. The corrosion protection of steel in 1M HCl using ODPEG-TS was investigated by different electrochemical techniques. Potentiodynamic polarization data revealed that the ODPEG-TS behaves as a mixed-type inhibitor influencing both the anodic dissolution and cathodic reactions. The protection performance of the ODPEG-TS inhibitor increased with increasing its concentrations. The inhibition action of ODPEG-TS occurred by adsorption of ODPEG-TS inhibitor on the active sides of steel surface according to Langmuir adsorption isotherm.

Keywords: Steel; Adsorption; Surface activity, Ionic liquid; Acid corrosion inhibitor.

1. INTRODUCTION

Corrosion in petroleum and gas oilfields causes large cost and energy losses all over the world. Moreover, the methods applied to control corrosion are used to avoid many hazardous and disasters that affect the air and water environmental pollutions. It is well known that the all oilfield operation stages from downhole to processing facilities can cause leaks in operation equipment such as pipelines, tanks, tubes, separators and other processing facilities based on steel [1-4]. The corrosion problems lead to process shutdown and reflect in serve economic losses [5]. There are several sources for corrosion in the petroleum and gas oilfields such as CO₂, H₂S, organic-sulfur, acids, formation water

and salts [5]. These aggressive environments are responsible for several types of corrosion, such as general and localized, stress, galvanic, erosion and crevice corrosions, which cause damage in the processing and transportation equipments [6-8]. The corrosion inhibitors became one of the most favorable and applicable technique among several methods used to control corrosion of steel in acidic environment [9-11]. The materials used to inhibit the effectiveness of the acid corrosion of steel at elevated temperatures are based on natural water soluble products, surfactants, and intensifiers [9]. Inhibitors contain nitrogen and phosphorous attracted great attention to apply as corrosion inhibitors due to their affinity to form a film on the metal surface. The produced film retarded dissolution (an anodic reaction) and hydrogen evolution (a cathodic reaction) on the steel surface at elevated temperatures [9]. There are several disadvantages produced from application of these materials as corrosion inhibitors such as toxicity, low thermal stability and volatility. Accordingly, these potential problems and disadvantages directed the researchers to produce green safer and environmentally more acceptable material.

The corrosive environments in the petroleum and gas oil field challenge the researcher to design of an efficient inhibitors. Ionic liquids (ILs) attracted great attention last decades as corrosion inhibitors due to their low toxicity, low volatility, high thermal stability, high ionic conductivity and high performance as corrosion inhibitors [12-16]. Another merit of ILs that exhibited negligible electrochemical processes between -2.5 V and 2.0 V which advances them to stand out as promising electro-chemical materials [17]. Moreover, the high ion concentrations of ILs used to replace water or any active small ions that create reactive environment during application of ILs as corrosion protective for reactive metals [18]. Last but not least, it is reported that the ILs can be applied as protective coats for metal substrates without pretreatment which opposed the most conventional coatings [19]. Moreover, the chemical structure of ILs and on the amount of water in ILs are important parameters to select them as protective coats for steel [15]. The net ILs showed great corrosion resistance at high temperatures and with decrement the amount of water used as solvent for ILs. The increment of water solvent produced corrosive ions that required adding new corrosion inhibitors to ILs contain water [15]. Imidazolium salts and their derivatives were performed to be the most efficient inhibitors for different metals at various corrosive conditions of carbon steel in the petroleum and gas oilfields [20-25]. It was also reported that quaternary ammonium salts ILs can be used as the corrosion initiators for steel in the oilfield [26]. The objective of the present work is to synthesize new IL derived from ethoxylated octadecylamine salts with p-toluene sulfonate. Moreover, the inhibition action of the prepared IL in 1 M solutions of HCl on the carbon steel at room temperature is investigated. The corrosion inhibition efficiencies of the IL were determined at different concentrations using electrochemical tests. Scanning electron microscopy (SEM) was used to evaluate the corrosion inhibition mechanism at the steel surface after exposure to the acid solution.

2. EXPERIMENTAL

2.1. Materials

Octadecylamine (ODA), P-toluene sulfonic acid monohydrate (PTSA; 99.5%) and 2,2-dichlorodiethyl ether (DDE), and poly(ethylene glycol) with molecular weight 1000 g/mol (PEG-1000),

were purchased from Aldrich Chemicals Co. Hydrochloric acid (37 wt%) was obtained from Merck Co. Steel specimens with chemical composition (weight %) 0.14% C, 0.57% Mn, 0.21% P, 0.15% S, 0.37% Si, 0.06% V, 0.03% Ni, 0.03% Cr and the balance Fe were used for the experiments. The working electrode was polished with different grades of emery paper, then washed in bi-distilled water, degreased ultrasonically in ethanol, and eventually dried.

2.2. Synthesis procedure:

Ethoxylation of ODA was carried out by reacting 0.05 mol of ODA (13.47 g) with 0.1 mol of PEG-1000 (100g) in the presence of 0.1 mol (14.3 g) of DDE as linking agent, 0.2 mol (8 g) of NaOH and 270 ml of xylene as a solvent in 500 ml round flask. The reaction mixture was refluxed for 5 hrs in the N₂ atmosphere. The reaction mixture was filtered to remove NaCl. Xylene solvent was removed by evaporation under vacuum. The product of ethoxylated octadecylamine was abbreviated as ODPEG.

Equal mol amounts of ODPEG and p-toluene-sulfonic acid were refluxed for 24 h under stirring and nitrogen gas atmosphere at temperature 145 °C. Finally, the product of ethoxyoctadecylammonium tosylate (ODPEG-TS) was obtained after cooling to room temperature. The melting temperature of ODPEG and ODPEG-TS salt are 32-34 and 48-50 °C, respectively.

2.3. Characterization:

¹H- and ¹³CNMR spectra of the prepared polymers were recorded on a 400MHz Bruker Avance DRX-400 spectrometer. D₂O is used as solvent for the prepared materials.

Contact angles and surface tension measurements were determined by using drop shape analyzer model DSA-100 at 25 °C. The surface tension measurements were carried out using pendant drop method. The equilibrium surface tension was determined from five measurements. The dynamic contact angle was measured between the aqueous solutions of the prepared materials and the steel surface (used for corrosion inhibition measurements) using sessile drop technique. The steel specimen was cleaned to obtain smooth steel surface. The needle of the instrument is located close to the steel surface and the volume of the droplet is gradually increased while recording at the same time of . The advancing contact angle was measured used to study the effect of ageing time on contact angle for different concentrations of the prepared materials.

Scanning electron microscope (SEM; Model JEOL-JSM-5400) was used to scan the steel microstructure.

2.4. Electrochemical measurements

Potentiodynamics experiments as well EIS measurements were carried out using a Solartron 1470E system (Potentiostat/ Galvanostat) with Solartron 1455A as FRA. A platinum sheet and SCE were used as a counter and as a reference electrode, respectively. Potentiodynamic polarization

studies were conducted with a scan rate of 1 mV/s. Electrochemical impedance spectroscopy (EIS) measurements were performed over a frequency range of 10 kHz - 0.01 Hz.

3. RESULTS AND DISCUSSION

Modified fatty amines attracted great attention due to their unique adsorption at different interfaces [27-29]. The chemical structure of modified amines plays important factor for their performance at interfaces [30]. The adsorption ability of amines at interfaces is affected by ability of nitrogen atoms to donate their electrons at interfaces which sterically hindered by the attached alkyl group. In this work, the effects of the chemical modification of ODA with ethoxylation followed by formation of organic salt on the surface properties of ODA and its corrosion inhibition ability in the acidic medium will be investigated. The reaction route is illustrated in the scheme 1. The preparation of IL from ODA is preceded by ethoxylation of amine group with PEG using DDE as linking agent followed by the interaction of a free electron pair in amine groups with H^+ of PTSA. However, ODPEG-TS as IL is prepared effectively in the absence of solvent as described in the experimental section.

The molecular structure of ODPEG and ODPEG-TS salt was characterized by NMR spectroscopy. The 1H NMR spectrum of ODPEG-TS is selected and represented in Fig. 1.

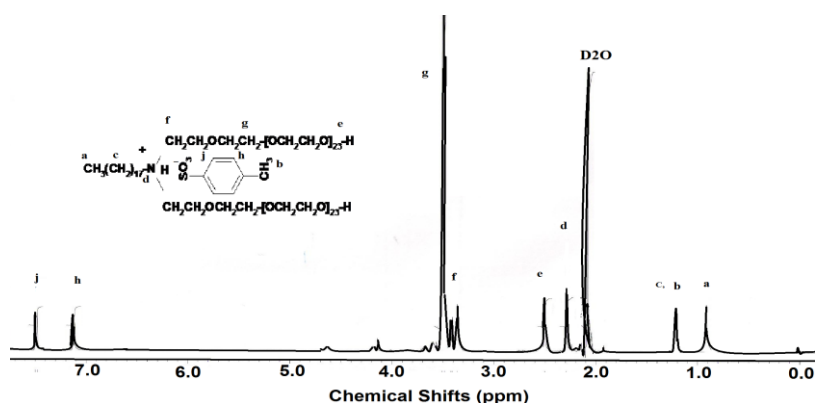


Figure 1. 1H NMR spectrum of ODPEG-TS.

The quaternization of ODPEG with PTSA to form ODPEG-TS can be confirmed from appearance of phenyl peaks, at chemical shifts (δ) 7.709 (doublet, 2H, $J = 8.1$ Hz), and 7.24 ppm (doublet of doublet, 2H, $J = 8.4, 0.6$ Hz, HW) as represented in Figure 1 [29]. The phenyl protons appeared at 7.709 ppm are de-shielded by electron withdrawing sulfonate anion and its repulsion with positive ammonium cation. The OH protons of PEG were exchanged with the solvent (D_2O) and be seen as a solvent peak DHO at 4.8 ppm. Moreover, the appearance of peak at 3.78 ppm, confirmed OCH_2CH_2 - peak, indicates the ethoxylation of ODA with PEG. The peaks at 3.692 (triplet, 2H, $J = 6.9$ Hz) and 2.374 ppm (singlet, 1H) represented the CH_2-N and ^+NH , respectively confirm the formation of ODPEG-TS salt. The peak at 2.5 ppm confirms the presence of $-OH$ group at PEG ends. The peaks

at 1.290 (multiplet), and 0.902 ppm (triplet, 3H, $J = 6.6$ Hz) represented to $(\text{CH}_2)_{16}$, CH_3 attached to phenyl of PTSA, and CH_3 of ODA respectively confirm the presence of alkyl chains of ODA and PTSA without degradation.

^{13}C NMR spectrum of ODPEG-TS (Fig. 2) showed peaks at $\delta = 142.63$, 139.86, 128.99 and 125.09 ppm which confirm phenyl and C-N carbons, respectively. The peaks at 77.72, 61.23, 30.77, 29.69, 29.39, 28.72, 27.60, 29.16, 22.49 and 13.61 ppm in spectrum of ODPEG-TS confirm the presence of OCH_2 , N-CH_2 , CH_2 and CH_3 carbons of PEG and ODA (Fig. 2) [29].

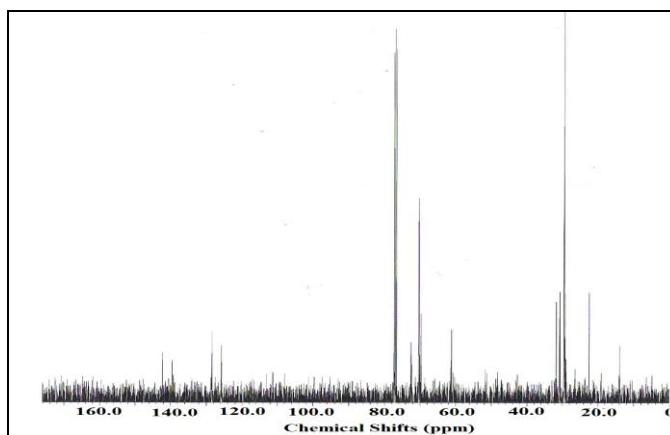


Figure 2. ^{13}C NMR spectrum of ODPEG-TS.

3.1. Surface properties of ODPEG and ODPEG-TS at Air/water interface

Adsorption of the materials capable to form self-assemble layer, at the interface, plays great importance in modern technology [31]. The presence of different active sites in the chemical structure of organic compounds such as surfactants, ionic liquids and polyelectrolytes affects their performance in aqueous solution [32-34]. Different techniques have been used to study the adsorption of the materials at interfaces [35-37]. The relation between surface tension data of ODPEG and ODPEG-TS at different concentrations used to determine the aggregation and adsorption parameters. In this respect, the relation between the equilibrium surface tension data (γ ; mN/m) of ODPEG and ODPEG-TS and their concentrations ($\ln c$, mol / L) at 25 °C is represented in Fig. 3.

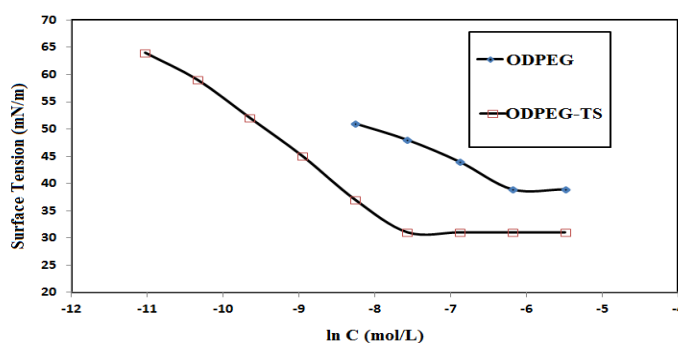


Figure 3. Relation between surface tension and different concentrations of ODPEG or ODPEG-TS at 25 °C.

The surface tension value was determined as average of five measurements. The differences between measurements were determined as ± 0.2 mN/m. The relation between the equilibrium time and surface tension measurements, not presented for brevity, reveal that the ODPEG-TS reaches equilibrium and adsorbs very fast at the interface more than ODPEG. The time required to reach equilibrium for γ measurements increases with dilution of ODPEG-TS concentrations. The equilibrium time was ranged from 3 to 15 minutes for ODPEG and reduced to 1 - 10 minutes for ODPEG-TS. The decrement of aging time of ODPEG-TS more than ODPEG to reach equilibrium indicates that the formation of quaternary amine salt and incorporation of tolyl group of PTSA are driving force for adsorption of ODPEG-TS at interface more than ODPEG. The presence of sulfonate group in the chemical structure of ODPEG-TS beside hydrophobic interactions at air/water interface affect the coiling of PEG at interface. The critical micelle concentrations (cmc; mol / L), determined at the concentration that γ is started to increase, and the corresponding surface tension at cmc (γ_{cmc}) are detected and tabulated in Table 1.

Table 1. Surface activity parameters of ODPEG and ODPEG-TS concentrations in water at 25 °C.

Derivatives	Cmc x 10 ⁴ (mol.L ⁻¹)	γ_{cmc} mN.m ⁻¹	π_{cmc} mN/m	$-\partial \gamma / \partial \ln c$	Γ_{max} x 10 ¹⁰ mol/ cm ²	A _{min} nm ² / molecule
ODPEG	20.73±0.3	39.2±0.2	33	5.77	2.33	0.71
ODPEG -TS	4.84±0.5	31.2±0.4	41	9.81	3.97	0.42

A complete understanding of the interaction between ODPEG -TS or ODPEG active sites with water requires knowledge of the entire spectrum of self-assembly. It is expected that the incorporation of two PEG having molecular weight 1000 g/mol increases the solubility of ODPEG through hydrogen bond formation with water. The data indicated that cmc and γ_{cmc} are reduced more for ODPEG -TS than ODPEG. This means that the formation of salt and incorporation of hydrophobic toluene moiety of IL ODPEG -TS affected their adsorption and aggregation in water [38]. A possible explanation for reduction of the water surface tension using ODPEG -TS seems reasonable to propose that the hydrophobic group of PTSA unfolding of surface tails and loops to cover the entire interface [38]. Furthermore, the location of charged moieties at the surface affects the aggregation of molecules in aqueous solution [39-41]. Accordingly, the presence of sulfonate at the outer surfaces of ODPEG -TS increases their interaction with water and greatly reduces the water surface tension. The interactions between ODPEG -TS or ODPEG and water are the main reason for the orientation and packing of surfactants at the air/water interface. The presence of charges for ODPEG -TS rearranges the molecules to adapt a flexible loop-like conformation with water either at interface or with aggregate.

The adsorption of ODPEG -TS or ODPEG molecules at air/water interface is the alternative mechanism to prevent their micellization in the bulk solution. The ability of molecules to adsorb at air / water interface used to evaluate their surface activities. The concentration of ODPEG -TS or ODPEG

molecules adsorbed per unit area of interface is designated as surface excess concentration (Γ_{\max}). It can be calculated from the relation: $\Gamma_{\max} = 1/RT \times (-\partial \gamma / \partial \ln c)_T$; where R and T are constant equals 8.314 J mol⁻¹ K⁻¹ and temperature (K) of measurements, respectively. The relation between A_{\min} and Γ_{\max} ($A_{\min} = 10^{16} / N \Gamma_{\max}$) where N is Avogadro's number. is used to calculate A_{\min} which summarized in Table 1. The A_{\min} was used to determine the orientation and packing degrees of the adsorbed ODPEG -TS or ODPEG, at the interfaces. Various parameters such as molecular interactions and surface coverage of the surfactants affect the effectiveness of surfactant to modify the surface tension and adsorption at interfaces. Moreover, different inter- and intra-molecular interactions of the amphiphiles at the interface are very important for stabilization of molecules at interfaces [42, 43]. The increment of Γ_{\max} value for ODPEG -TS, Table 1, indicated the increment of ODPEG -TS concentration adsorbed at the air/ water interface which also reflected on a reduction of water surface tension. The increment of Γ_{\max} value for ODPEG -TS can be referred to the interactions between the hydrophilic arms of ODPEG -TS molecules that increase the packing of molecules at interfaces. The low A_{\min} (0.42 nm²/molecule) obtained for ODPEG -TS suggests adsorption of ODPEG -TS which oriented away from the liquid in a more tilted position. However, the complete surface coverage of ODPEG -TS chains with the flexible air/water interface were confirmed from low A_{\min} and high Γ_{\max} values.

3.2. Contact angle and surface free energy measurements

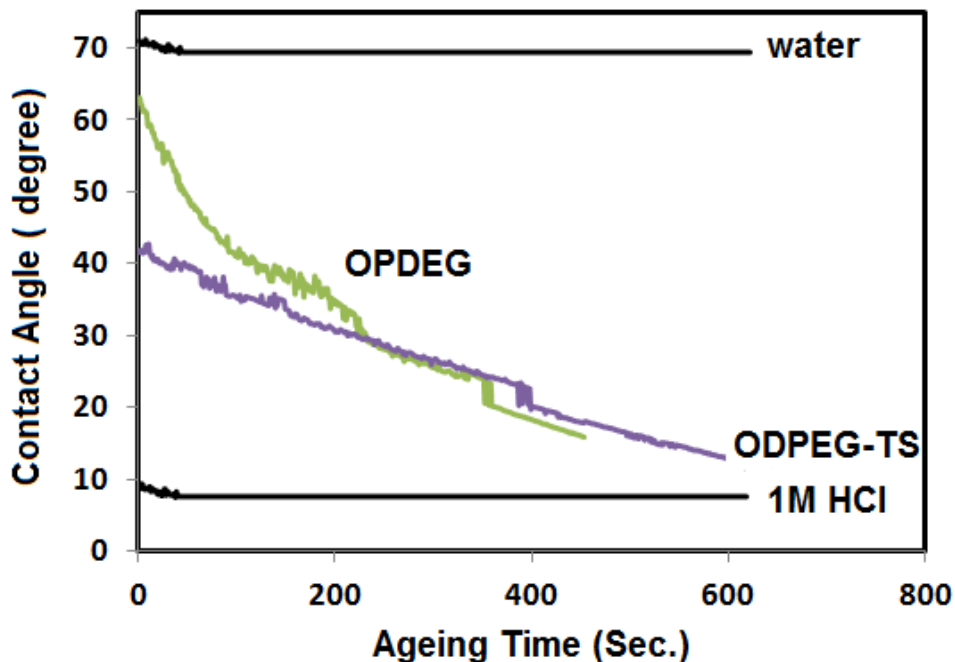


Figure 4. Relation between contact angles of aqueous solutions at the steel surface and ageing times using 2.1 mM of ODPEG and 0.48 mM of ODPEG-TS.

One of the interesting criteria which used to study the adsorption and wetting characteristics of the organic molecules on the surface of the steel is the advancing contact angle measurements. It is

used to determine the interactions and diffusion of molecules with the air and the substrate [44]. The wetting characteristics of steel in absence of corrosion inhibitor in acidic conditions were changed because its surface roughness was changed from the surface degradation of the steel [44]. The relation between the work of adhesion (WA) and contact angles (θ°) used to calculate surface free energy values (E) from Young Eqns. [44]:

$$WA = \gamma (1 + \cos \theta^\circ) \tag{1}$$

$$WA = 2(\gamma \times E)^{1/2} \exp [-\beta (\gamma - E)^2] \tag{2}$$

Where γ is the surface tension of aqueous 1M HCl solution in the absence and presence of ODPEG -TS or ODPEG molecules while the value of β is $0.0001247 \pm 0.000010 \text{ (mJ/m}^2\text{)}^{-2}$ [44]. The relation between contact angle and ageing time is illustrated in Fig. 4. The relation between the contact angle values and the concentrations of ODPEG -TS or ODPEG is represented in Fig. 5.

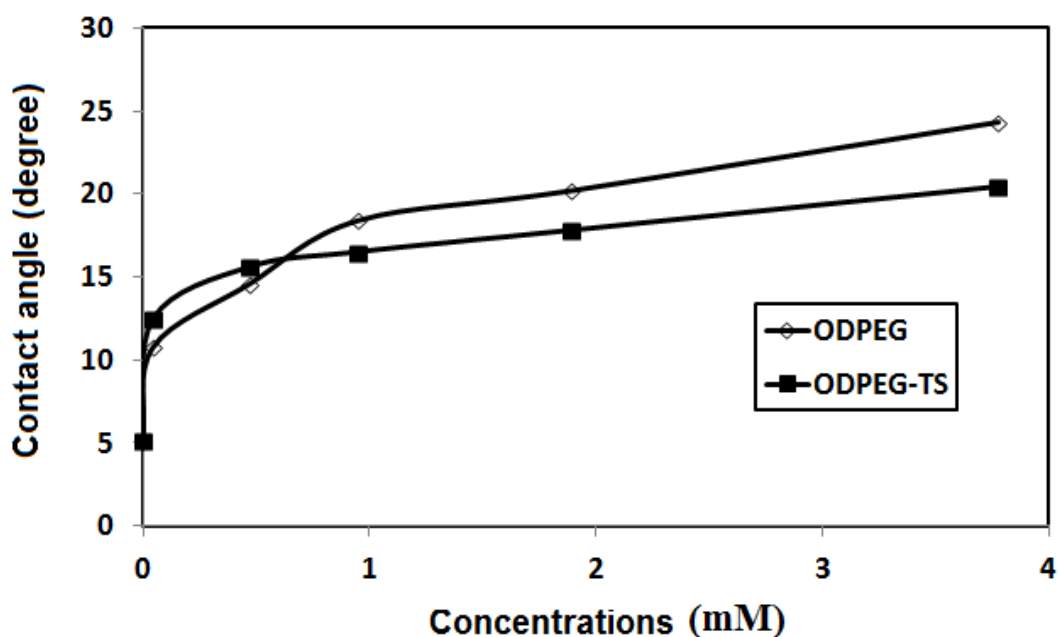


Figure 5. Relation between contact angles of ODPEG and ODPEG-TS and their concentrations at 25 °C.

The contact angle measurements between steel and water or aqueous 1M HCl solution (Fig. 4) achieve stable measurements with ageing times. The ageing times of 1M HCl in the absence and presence of different concentrations of the ODPEG -TS or ODPEG to reach the stable contact angles at steel surface were measured and listed in Table 2. Moreover the contact angle between steel and water is higher than that determined in 1M HCl. This indicates the presence of higher interactions between steel and HCl that causes degradation and steel corrosion. The contact angles increased with increase ODPEG -TS or ODPEG concentrations with the reduction of ageing times (Fig. 4, 5 and Table 2) that indicates the increment of their adsorption at steel substrate. The E values of steel were calculated in absence and presence of ODPEG -TS or ODPEG and gathered in Table 2. It was observed that the increment of ODPEG -TS or ODPEG concentrations reduces E values and increases contact angles between their solution and steel surfaces which attributed to increase steel surface hydrophobicity [45].

Table 2. Contact angle and surface free energy values of steel samples in different concentrations of ODPEG and ODPEG-TS of 1 M HCl solutions.

Concentrations (mM)	E (mJ/m ²)				Ageing time (second)	
	ODPEG		ODPEG-TS		ODPEG	ODPEG-TS
	Accurate value	S.D.	Accurate value	S.D.		
0	25.1±0.3	0.21	25.1±0.3	0.21	30	30
3.774	10.8±0.8	0.63	12.5±0.6	0.42	20	10
1.895	14.6±0.9	0.65	15.6±0.5	0.44	200	100
0.951	18.4±0.6	0.52	16.5±0.4	0.38	400	300
0.471	20.2±0.4	0.44	17.8±0.3	0.36	650	600
0.045	24.3±0.2	0.12	20.4±0.1	0.06	900	800

3.3. Potentiodynamic Polarization Measurements

The anodic-cathodic polarization curves of steel electrode in 1M HCl solutions containing different of concentrations of ODPEG and ODPEG-TS are shown in in Figs. 6 a and b, respectively.

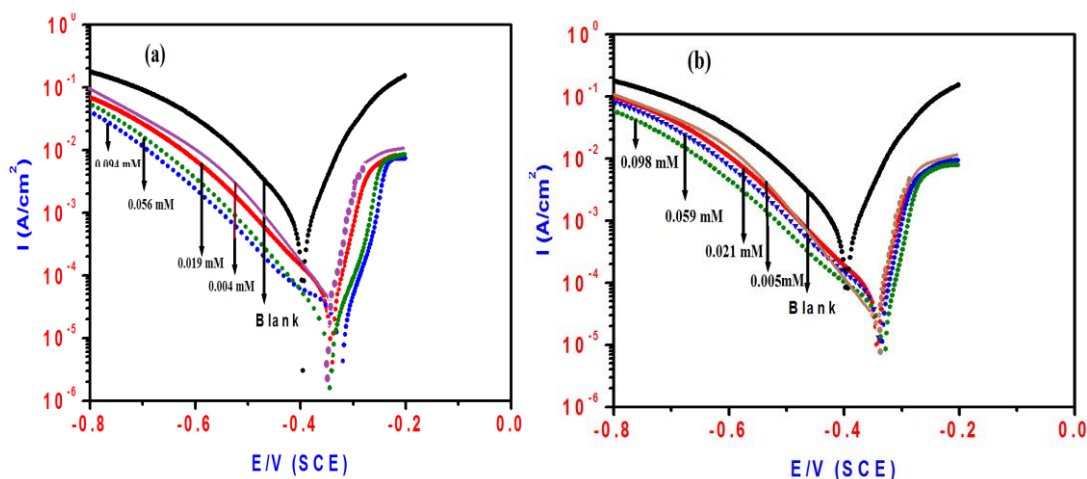


Figure 6. Potentiodynamic curves of steel electrode using saturated calomel electrode (SCE) as reference electrode in 1M HCl solution with different concentrations of a) ODPEG and b) ODPEG-TS.

It can be seen that the additions of ODPEG and ODPEG-TS influenced both the anodic and the cathodic current density (Figs. 6 a and b), which lowered the corresponding potential. The noble shift in the potential with the additions of ODPEG and ODPEG-TS suggests that the protection action of such compounds occurs by blocking the active sides of steel surface via adsorption [46-47]. It can be

seen also from the plots shown in Figs. 6a and b that the addition of both compounds suppressed both the anodic and cathodic reactions of the steel. It was reported previously that if the displacement in the corrosion potential is more than 85mV in cathodic or anodic direction with respect to the blank solution the inhibitor is known as cathodic or anodic type [48–50]. Otherwise inhibitor is labeled as a mixed type. The maximum displacement in our investigation was found to be less than 85mV in both inhibitors. This result indicates that the additives behaved as a mixed-type inhibitor by retarding the anodic and cathodic reactions. It can be concluded that the inhibition process is probably due to adsorption of inhibitor on the active sites of the steel surface and formation of protective layer, which blocks the available reaction sites and acts as barrier for diffusion and attacking the aggressive ions [49]. All the electrochemical parameters obtained from the potentiodynamic polarization curves are given in Table 3 and 4 for ODPEG and ODPEG-TS, respectively.

Table 3. Inhibition efficiency values of steel electrode in 1M HCl containing various concentrations of the and ODPEG calculated by polarization and EIS methods.

Concentrations mM	Polarization Method					EIS Method		
	Ba (mV)	Bc (mV)	E _{corr} (V)	i _{corr} μA/cm ²	IE%	R _{ct} Ohm	Cdl (μF/cm ²)	IE%
Blank	69	120	-0.3955±0.003	839±0.03	_____	1.80	334	_____
0.004	75	111	-0.355±0.001	147±0.04	82.4±0.1	10.5	134	82.8±0.1
0.019	58	137	-0.3411±0.002	63±0.01	92.4±0.3	24	105	92.5±0.3
0.056	44	159	-0.3223±0.001	21±0.02	97.4±0.2	73	93	97.5±0.2
0.094	47	97	-0.3433±0.003	14±0.01	98.3±0.1	99	89	98.2±0.1

Table 4. Inhibition efficiency values of steel electrode in 1M HCl containing various concentrations of the and ODPEG-TS calculated by polarization and EIS methods

Concentrations mM	Polarization Method					EIS Method		
	Ba (mV)	Bc (mV)	E _{corr} (V)	i _{corr} μA/cm ²	IE%	R _{ct} Ohm	Cdl (□F/cm ²)	IE%
Blank	69	120	-0.3955±0.003	839±0.03	_____	1.80	334	_____
0.005	68	108	-0.360±0.001	89±0.01	89.3±0.1	17.6	114	89.7±0.1
0.021	62	151	-0.3416±0.003	99±0.01	88.2±0.3	15.8	114	88.6±0.3
0.059	52	106	-0.3414±0.002	34±0.01	95.9±0.2	45	102	96±0.2
0.098	48	124	-0.3336±0.001	29±0.01	96.5±0.1	55	100	96.7±0.1

The IE (%) was computed using the expression [51]:

$$IE\% = (1 - i_{corr(inh)} / i_{corr}^o) * 100 \tag{3}$$

Where $i_{\text{corr (inh)}}$ and i_{corr}° are corrosion current densities in the presence and absence of inhibitor, respectively. The values of IE% with different inhibitor concentrations are listed in Table 3 and 4 ODPEG and ODPEG-TS, respectively. Data in the tables 3 and 4 show that IE increased as ODPEG and ODPEG-TS concentration increased. The higher of the inhibitor concentration means the higher the surface coverage of the inhibitor molecules on the steel surface.

3.4. EIS measurements

The electrochemical processes occurring at the steel/solution interface resulted from the additions of ODPEG and ODPEG-TS can be investigated by EIS studies. The Nyquist plots for the impedance response of the steel in 1M HCl solution containing different concentrations of ODPEG and ODPEG-TS are shown in Figs. 7 a and b, respectively. Two different symbols as dots and squares, Figs 7a and b, are used to identify the accuracy between fit data and experimental data, respectively. Additions of the inhibitor to the acidic chloride solution leads to an increase in the diameter of the capacitive semicircle plot indicating that the corrosion process was mainly controlled by charge transfer reaction[52]. EIS data were appropriately fitted by a circuit model shown in Figure 8.

This model has been previously employed for fitting the steel/solution interface [53]. The values of the electrochemical parameters in the absence and presence of ODPEG and ODPEG-TS are given in Tables 3 and 4, respectively. It can be seen from the results presented in the Tables 3 and 4 that the addition of ODPEG and ODPEG-TS resulted in a reduction in the values double layer capacitance (Cdl) and an increase in charge transfer resistance values (Rct), which is in agreement with the diameter enlargement of the capacitive loop shown in Figs. 7a and b.

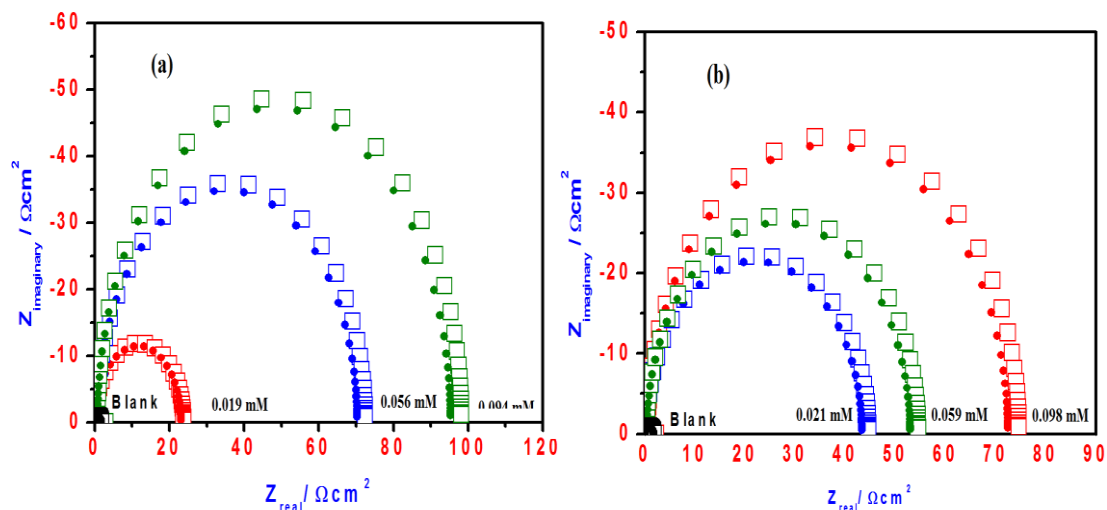


Figure 7. Nyquist plots of steel electrode obtained in 1M HCl solution and containing various concentrations of a) ODPEG and b) ODPEG-TS.

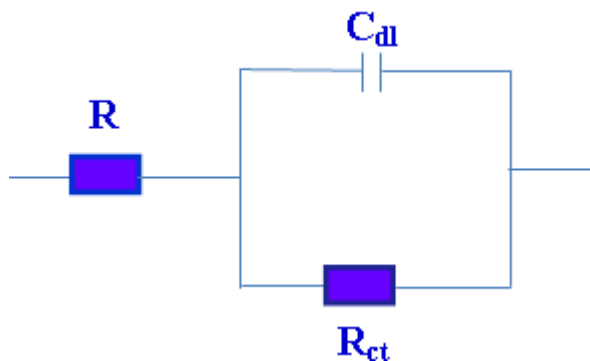


Figure 8. Equivalent circuit used for fitting the impedance data in 1 M HCl solution.

The thickness of the Cdl layers along with the amount of adsorbed molecules increased with increasing inhibitor concentrations [54]. Inhibition efficiency (IE%) was estimated from the impedance data as follows:

$$\text{IE\%} = [1 - (R_{ct}^1/R_{ct}^2)] \times 100 \quad (4)$$

Where (R_{ct}^1) is the charge transfer resistance in the absence of inhibitor and (R_{ct}^2) is the charge transfer resistance in the presence of inhibitor. The values of IE% increase with increasing inhibitor concentration, which suggests an adsorption of the inhibitor molecules on the steel surface with a formation of an inhibitive layer. The higher the R_{ct} values, the slower the corrosion process. The formed inhibitive film hinders the diffusion of aggressive ions to the steel surface and causes a decrease in R_{ct} values in presence of inhibitor. The replacement of water molecules with charged inhibitor molecules leads to a decrease in the values of Cdl[55].

3.5 Adsorption isotherm

The interaction arises from the adsorption of the inhibitor and the exposed surface can be investigated for studying the different adsorption models [56]. The experimental data was found to be fitted by Langmuir's adsorption isotherm. The relation between surface coverage θ and the inhibitor concentration is given by Langmuir's adsorption isotherm [57]:

$$C_{(\text{inh})} / \theta = 1/K_{\text{ads}} + C_{(\text{inh})} \quad (5)$$

where $C_{(\text{inh})}$ is the inhibitor concentration, K_{ads} is the adsorption equilibrium constant and θ is the surface coverage. The surface coverage, θ , was calculated using the following equation:

$$\theta = 1 - (i / i_{\text{corr}}^0) \quad (6)$$

where, i and i_0 represent the corrosion current densities of steel electrode in the presence and absence of inhibitors, respectively. Fig. 9a and b shows the plot of $C_{(\text{inh})} / \theta$ against C for steel in 1M HCl solution in the presence of ODPEG and ODPEG-TS, respectively. The linear plots of the experimental results indicate that the adsorption of both inhibitors can be fitted by the Langmuir adsorption isotherm. The plots obtained for ODPEG and ODPEG-TS are linear, with slopes of 1.004 and 1.008, respectively. This indicates that adsorption of both inhibitors follows the Langmuir

adsorption isotherm. The strong correlation values ($R^2 = 0.9999$) obtained at both inhibitors indicates the applicability of Langmuir adsorption isotherm. The standard free energy of adsorption, ($\Delta G^\circ_{\text{ads}}$) can be calculated from K_{ads} as [58]:

$$\Delta G^\circ_{\text{ads}} = -RT(\ln 55.5K_{\text{ads}}) \quad (7)$$

Where R is the gas constant ($8.314 \text{ J mol}^{-1} \text{ K}^{-1}$), and T is the absolute temperature (K). The larger the negative values of $\Delta G^\circ_{\text{ads}}$ the higher the stability of the adsorbed layer of the inhibitor on the metal surface [59-61]. The high negative value of adsorbed $\Delta G^\circ_{\text{ads}}$ indicated the high stability of the adsorbed film [59-61]. It is established well that values the values of $\Delta G^\circ_{\text{ads}}$ determines the type of adsorption. The inhibitor was physically adsorbing on the exposed surface when the values around -20 kJ mol^{-1} or below. The chemisorption mechanism is predominant process when the values around -40 kJ mol^{-1} or higher with a formation a co-ordinate-type bond [62-64]. The values of $\Delta G^\circ_{\text{ads}}$ are estimated and found to be -35.78 and $-35.89 \text{ kJ mol}^{-1}$ for ODPEG and ODPEG-TS, respectively. Accordingly, the adsorption of ODPEG and ODPEG-TS on the steel surface occurs through both chemical and physical adsorption namely mixed type inhibitor [65].

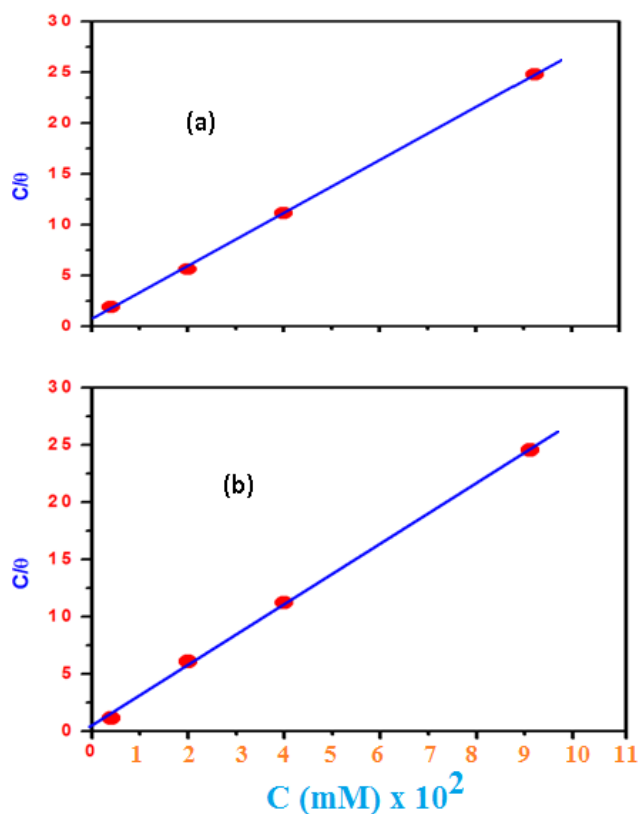


Figure 9. Langmuir adsorption plot of steel in 0.1 M HCl solution containing different concentrations of: (a) ODPEG and (b) ODPEG-TS.

3.6 Adsorption mechanism

SEM analysis used to investigate the interactions and damage occurred for steel surface with and without ODPEG-TS as inhibitor as illustrated in Fig. 10. Fig. 10a showed a damaged rough steel

surface without inhibitor. Fig. 10b showed a formation of uniform layer on the steel surface in the presence of 100 ppm of ODPEG-TS which indicates the adsorption of inhibitor on the steel surface. Fig. 10 c represents a smooth surface which acts as an evidence for the corrosion inhibition of ODPEG-TS in 1M HCl by forming protective film on the steel electrode surface.

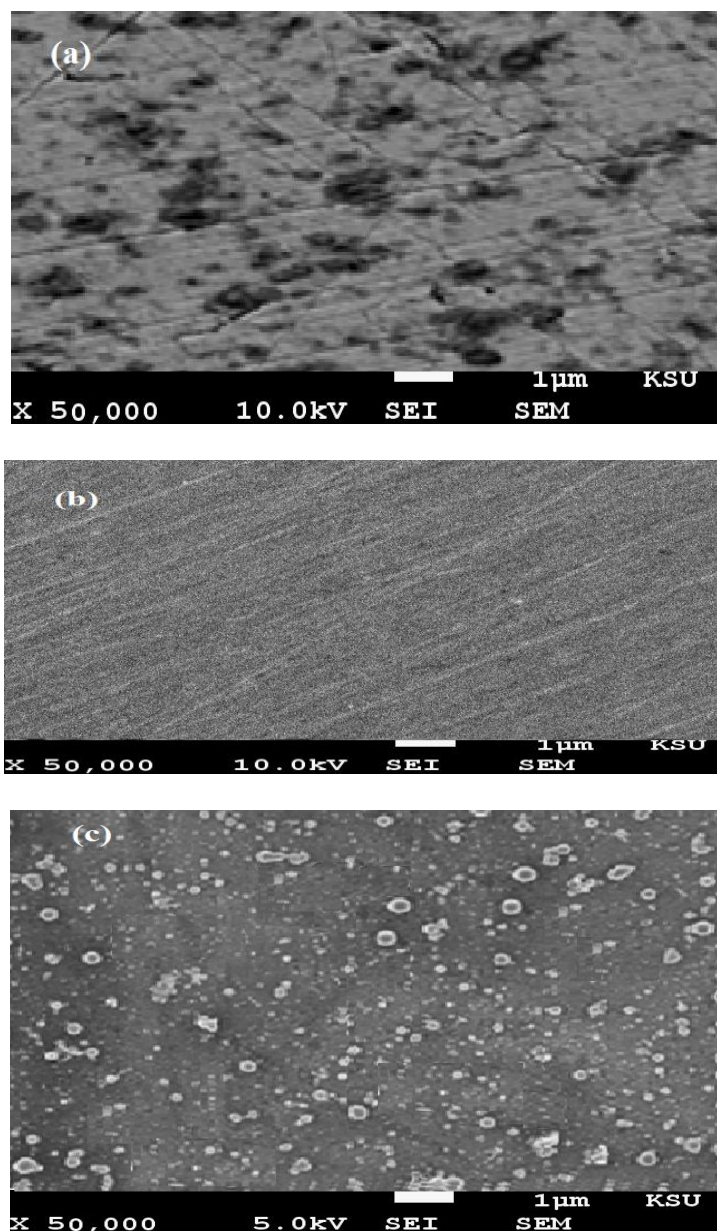


Figure 10. SEM micrographs of steel electrode a) without inhibitor in 1M HCl, the presence of 150 ppm of ODPEG-TS b) before and c) after immersion for 24 hrs in 1M HCl.

The mechanism of ODPEG-TS inhibition can be illustrated on the basis of adsorption of ODPEG-TS on the electrode surface. The ODPEG-TS inhibitor replaced adsorbed water molecules and chloride ions by forming stable thin layers to inhibit the diffusion of chloride ions onto the steel surfaces. The electrochemical measurements indicated that the anodic and cathodic reactions were inhibited by the presence of ODPEG-TS or ODPEG compounds. The donor-acceptor interaction

mechanism between ODPEG-TS molecules and iron metal substrate is responsible for the chemical adsorption of inhibitors at the steel surface. In this respect, the presence of π orbital of phenyl, lone pair of electrons on the nitrogen, oxygen and sulfur heteroatoms of the ODPEG-TS or ODPEG molecules can act as donor and Fe^{2+} ions acts as acceptor. This chemical interaction between inhibitors and the surface of the metal is responsible for anodic inhibition reaction [66]. Moreover, the quaternary amine group exists in protonated form in the acidic medium increases the tendency to inhibit the cathode evolution of hydrogen. Accordingly, ODPEG-TS or ODPEG retard the corrosion of mild steel efficiently due to the presence of positive charge on quaternary ammonium group, phenyl π -orbital and lone pair of nitrogen, oxygen and sulfur electrons are responsible for formation of thin layers between steel surface and ODPEG-TS or ODPEG inhibitors.

4. CONCLUSIONS

(1) New synthesized amphiphilic ionic liquid based on ethoxylated octadecyl amine ODPEG-TS possesses good surface active properties.

(2) ODPEG and ODPEG-TS have good protection performance in the acid chloride containing environment and the protection performance increased with an increase in the ODPEG and ODPEG-TS concentration.

(3) Electrochemical results show that ODPEG and ODPEG-TS act as mixed-type inhibitor.

(4) EIS data display one capacitive loop whose diameter increase with increasing the ODPEG and ODPEG-TS concentration.

(5) Adsorption of ODPEG and ODPEG-TS onto steel surface following the Langmuir adsorption isotherm model.

ACKNOWLEDGEMENT

The project was financially supported by King Saud University, Vice Deanship of Research Chairs.

References

1. Z. Panossian, N. L. Almeida, R. M. Sousa, G. d. Pimenta and L. B. Marques, *Corros. Sci.*, 58 (2012) 1–11.
2. M. M. Osman and M. N. Shala, *Mater. Chem. Phys.*, 77 (2003) 261–269.
3. P. C. Okafor, X. Liu and Y. G. Zheng, *Corros. Sci.*, 51 (2009) 761–768.
4. S. Nesic and W. Sun, *Corrosion in Acid Gas Solutions*, Shreir's Corrosion, Oxford, Elsevier Science, (2010) 1270–1298.
5. V. Garcia-Arriaga, J. Alvarez-Ramirez, M. Amaya and E. Sosa, *Corros. Sci.*, 52 (2010) 2268–2279.
6. S. Ghareba and S. Omanovic, *Corros. Sci.*, 52 (2010) 2104–2113.
7. D. Martinez, R. Gonzalez, K. Montemayor, A. Juarez-Hernandez, G. Fajardo and M. A. Hernandez-Rodriguez, *Wear* 267 (2009) 255–258.
8. S. M. Wilhelm, *Corrosion* 48 (1992) 691–703.
9. M. Finšgar and J. Jackson, *Corros. Sci.*, 86 (2014) 17–41.

10. P. B. Raja and M. G. Sethuraman, *Mater. Lett.*, 62 (2008) 113–116
11. M. A. Malik, M. A. Hashim, F. Nabi and S. A. AL-Thabaiti, *Int. J. Electrochem. Sci.*, 6 (2011) 1927–1948.
12. G. A. El-Mahdy, A. M. Atta, H. A. Al-Lohedan, A. O. Ezzat, *Int. J. Electrochem. Sci.*, 10(2015)5812-5826.
13. A. M. Atta, G. A. El-Mahdy, H. A. Allohedan, M. M. S. Abdullah, *Int. J. Electrochem. Sci.*, 10(2015)6106-6119.
14. L. Anicai, A. Petica, S. Costovici, P. Prioteasa and T. Visan, *Electrochimica Acta*, 114 (2013) 868 – 877.
15. P. Huang, J-A. Latham, D. R. MacFarlane, P. C. Howlett and M. Forsyth, *Electrochimica Acta*, 110 (2013) 501– 510.
16. M. Uerdingen, C. Treber, M. Balsler, G. Schmitt and C. Werner, *Green Chemistry*, 7 (2005) 321-325.
17. M. Galinski, A. Lewandowski and I. Stepniak, *Electrochimica. Acta*, 51 (2006) 5567-5580.
18. P. C. Howlett, N. Brack, A. F. Hollenkamp, M. Forsyth and D. R. MacFarlane, *J. Electrochem. Soc.*, 153 (2006) A595-A606.
19. M. Forsyth, P. C. Howlett, S. K. Tan, D. R. MacFarlane and N. Birbilis, *Electrochem. Solid-State Lett.*, 9 (2006) B52-B55.
20. M. A. Quraishi, M. Z. Rafiquee, S. Khan and N. Saxena, *J. Appl. Electrochem.*, 37 (2007) 1153-1162.
21. M. Cai, Y. Liang, F. Zhou and W. Liu, *ACS Appl. Mater. Interfaces*, 3 (2011) 4580-4592.
22. S. Caporali, A. Fossati, A. Lavacchi and I. Perissi, *Corros. Sci.*, 50 (2008) 534-539.
23. P. Zhao, C. Zhong, L. Hunag, L. Niu and F. Zhang, *Corros. Sci.*, 50 (2008) 2166-2171.
24. H. Ashassi-Sorkhabi and M. Eshaghi, *Mater. Chem. Phys.*, 114 (2009) 267-271.
25. G. Yue, X. Lu, Y. Zhu, X. Zhang and S. Zhang, *Chem. Eng. J.*, 147 (2009) 79-86.
26. P. Bonhôte, A-P. Dias, N. Papageorgiou, K. Kalyanasundaram and M. Grätzel, *Inorg. Chem.*, 35 (1996) 1168-1178.
27. H. Choi, K. Y. Kim and J. M. Park, *Prog. Org. Coat.*, 76 (2013) 1316–1324.
28. M. A. Hegazy, M. Abdallah, M. K. Awad and M. Rezk, *Corros. Sci.*, 81 (2014) 54–64.
29. A. M. Atta, H. A. Al-Lohedan, M. M.S. Abdullah, S. M. ElSaeed, *Journal of Industrial and Engineering Chemistry, In Press, Corrected Proof, Available online 1 October 2015*, doi:10.1016/j.jiec.2015.09.028.
30. H. M. Bhajiwala and R. T. Vashi, *Bull. Electrochem.*, 17 (2001) 441–448.
31. R. R. Costa and J. F. Mano, *Nanomaterials in Tissue Engineering*, (2013) 88-118.
32. D. Mecerreyes, *Prog. Polym. Sci.*, 36 (2011)1629-1648.
33. M. Tamaddondar, H. Pahlavanzadeh, S. S. Hosseini, G. Ruan and N. R. Tan, *J. Membr. Sci.*, 472 (2014) 91-101.
34. J. Lu, F. Yan and J. Texter, *Prog. Polym. Sci.*, 34 (2009) 431-448.
35. L. Wang, C. Zhao, M. H. Duits, F. Mugele and I. Siretanu, *Sens. Actuators, B* 210 (2015) 649-655.
36. A. E. Thomsen, H. Jensen, L. Jorgensen, M. de Weert and J. Østergaard, *Colloids Surf., B* 63 (2008) 243-248.
37. V. Mitropoulos, A. Mütze and P. Fischer, *Adv. Colloid Interface Sci.*, 206 (2014) 195-206.
38. M. J. Rosen, *Surfactants and Interfacial Phenomena*. New York: *John Wiley and Sons* (1978).
39. S. Schachschal, A. Balaceanu, C. Melian, D. E. Demco, T. Eckert, W. Richtering and A. Pich, *Macromolecules*, 43 (2010) 4331–4339.
40. A. Pich, A. Tessier, V. Boyko, Y. Lu and H-J. Adler, *Macromolecules*, 39 (2006) 7701–7707. J. Kleinen and W. Richtering, *Colloid Polym. Sci.*, 289 (2011) 739–749.
41. S. Arditty, V. Schmitt, J. Giermanska-Kahn and F. Leal-Calderon, *J. Colloid Interface. Sci.*, 275 (2004) 659–664.
42. B. P. Binks, P. D. Fletcher and S. N. Kotsev, *Langmuir*, 13 (1997) 6669–6682.

43. D. Li and A. W. Neumann, *J. Colloid Interface, Sci.*, 137 (1990) 304–307. J. T. Woodward, H. Gwin and D. K. Schwartz, *Langmuir*, 16 (2000) 2957–2961.
44. A. Popova, *Corros. Sci.*, 49 (2007) 2144–2158.
45. A. Chetouani, M. Daoudi, B. Hammouti, T. Ben Hudda and M. Benkaddour, *Corros. Sci.*, 48 (2006) 2987–2997.
46. B. D. Mert, M. E. Mert, D. Kardaş and B. Yazıcı, *Corros. Sci.*, 53 (2011) 4265–4272.
47. B. S. Sanatkumar, J. Nayak and A. N. Shetty, *Int. J. Hydrogen Energy*, 37 (2012) 9431–9442.
48. W. H. Li, Q. He, S. Zhang, C. Pei and B. Hou, *J. Appl. Electrochem.*, 38 (2008) 289–295.
49. E. McCafferty, *Corros. Sci.*, 47 (2005) 3202–3215.
50. Q. Qu, L. Li, W. Bai, S. Jiang and Z. Ding, *Corros. Sci.*, 51 (2009) 2423–2428.
51. E. E. Oguzie, C. K. Enenebeaku, C. O. Akalezi, S. C. Okoro, A. A. Ayuk and E. N. Ejike, *J. Colloid Interface Sci.*, 349 (2010) 283–292.
52. E. E. Oguzie, Z. O. Iheabunike, K. L. Oguzie, C. E. Ogukwe, M. A. Chidiebere, C. K. Enenebeaku and C. O. Akalezi, *J. Dispers. Sci. Technol.*, 34 (2013) 516–527.
53. H. Wang, X. Wang, L. Wang and A. Liu, *J. Mol. Model*, 13 (2007) 147–153.
54. E. Machnikova, K. H. Whitmire and N. Hackerman, *Electrochim. Acta*, 53 (2008) 6024–6032.
55. E. Bayol, T. Gurtenb, A. A. Gurtena and M. Erbil, *Mater. Chem. Phys.*, 112 (2008) 624–630.
56. T. T. Qin, J. Li, H.Q. Luo, M. Li and N. B. Li, *Corros. Sci.*, 53 (2011) 1072–1078.
57. G. Avci, *Colloids Surf., A* 317 (2008) 730–736.
58. M. Abdallah, *Corros. Sci.*, 44 (2002) 717–728.
59. M. Lebrini, M. Lagrenée, M. Traisnel, L. Gengembre, H. Vezin and F. Bentiss, *Appl. Surf. Sci.*, 253 (2007) 9267–9276.
60. G. Moretti, F. Guidi and G. Grion, *Corros. Sci.*, 46 (2004) 387–403.
61. F. M. Donahue and K. Nobe, *J. Electrochem. Soc.*, 112 (1965) 886–891.
62. E. Khamis, F. Bellucci, R. M. Latanision and E. S. El-Ashry, *Corrosion* 47 (1991) 677–686.
63. G. E. Badr, *Corros. Sci.*, 51 (2009) 2529–2536.
64. L. Feng, H. Yang and F. Wang, *Electrochimica. Acta*, 58 (2011) 427–436.